



Cite this: *Chem. Commun.*, 2019, 55, 13578

Received 12th September 2019,  
Accepted 10th October 2019

DOI: 10.1039/c9cc07123g

rsc.li/chemcomm

## Facile assembly of bifunctional, magnetically retrievable mesoporous silica for enantioselective cascade reactions†

Zhongrui Zhao,‡ Fengwei Chang,‡ Tao Wang, Lijian Wang, Lingbo Zhao, Cheng Peng and Guohua Liu \*

**An integrated immobilization to encapsulate the Pd/C-coated magnetic nanoparticles within the chiral Ru/diamine-functionalized silica shell for the construction of a bifunctional magnetic catalyst is developed. This catalyst realizes a synergistic Suzuki cross-coupling/asymmetric transfer hydrogenation and a successive reduction/asymmetric transfer hydrogenation for the preparation of chiral aromatic alcohols.**

Increasing interest in the use of magnetically recoverable nanomaterials as heterogeneous catalysts has led to a wide range of applications in various efficient chemical processes being reported in the literature.<sup>1</sup> Numerous monofunctional magnetic catalysts have been focused on in single-step catalytic reactions, which involve the preparation of a variety of nonchiral<sup>2</sup> and chiral<sup>3</sup> organic molecules. Despite these significant achievements, the development of magnetically recyclable catalysts is still lagging behind compared to general nonmagnetic heterogeneous catalysts.<sup>4</sup> The main limitations lie in the challenging task of characterization, which brings a series of subsequent problems, for example, the deep understanding of the interactions of the active species and detailed elucidation of the role of the catalytic mechanism. In particular, the construction of a chiral bifunctional magnetic catalyst has not yet been explored, especially for application in a more complicated multi-step sequential enantioselective organic transformation. Reviewing the recent explorations reported to date, only a mesoporous silica-supported acid–base-bifunctional magnetic catalyst has been used to prepare nonchiral organic molecules *via* a deacetalization-Henry cascade reaction of benzaldehyde dimethyl acetal.<sup>5</sup> There is no doubt that the development of a chiral bifunctional magnetic catalyst and realization of an enantioselective cascade reaction are of great significance.

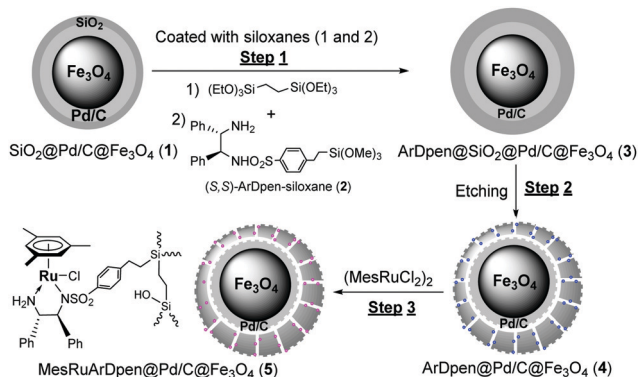
In the fabrication of bifunctional catalysts, yolk–shell-mesostructured silicas<sup>6</sup> possess a particular distinguishing feature, since the salient morphological structure is beneficial to anchor dual-species through the detachable yolk and shell, forming catalytically active site-isolated bifunctional catalysts. In particular, the outer shell layer in these yolk–shell-mesostructured silicas not only prevents magnetic aggregation, but also avoids the loss of the magnet, overcoming the traditional drawbacks of general magnetic catalysts. Thus, inspired by the constructions of yolk–shell-mesostructured heterobifunctional catalysts, it is reasonable to expect that a bifunctional magnetic catalyst could be easily assembled through the incorporation of magnetic Fe<sub>3</sub>O<sub>4</sub> into a yolk–shell-mesostructured silica network.

Based on our continued interest in the development of magnetic catalysts,<sup>7</sup> together with our recent experiences in the assembly of yolk–shell-mesostructured heterogeneous catalysts,<sup>8</sup> here we use an integrated immobilization strategy to encapsulate Pd/C-coated magnetic nanoparticles within a chiral Ru/diamine-functionalized silica shell, to construct a yolk–shell-mesostructured, site-isolated bifunctional magnetic catalyst. Our aim lies in the exploration of a feasible enantioselective cascade reaction. In this contribution, through utilization of the coupling or reductive ability of classic Pd/C nanoparticles,<sup>9</sup> together with an extensively studied asymmetric transfer hydrogenation (ATH) reaction,<sup>10</sup> we performed two types of sequential organic transformations, synergistic Suzuki cross-coupling/ATH and successive reduction/ATH cascade reactions. As presented in Scheme 1, a simple three-step procedure was used to assemble the bifunctional magnetic catalyst, abbreviated as MesRuArDpen@Pd/C@Fe<sub>3</sub>O<sub>4</sub> (**5**) (MesRuArDpen:<sup>11</sup> Mes = mesitylene, and ArDpen = (*S,S*)-4-(((trimethoxysilyl)ethyl)phenylsulfonyl)-1,2-diphenylethylenediamine (**2**)). Firstly, readily available SiO<sub>2</sub>-coated Pd/C-Fe<sub>3</sub>O<sub>4</sub> nanoparticles (**1**)<sup>12</sup> were coated *via* the condensation of **2** and 1,2-bis(triethoxysilyl)ethane to afford ArDpen@SiO<sub>2</sub>@Pd/C@Fe<sub>3</sub>O<sub>4</sub> (**3**). Selective etching of the sandwiched SiO<sub>2</sub>-coated layer then gave ArDpen@Pd/C@Fe<sub>3</sub>O<sub>4</sub> (**4**). Finally, the reaction of **4** and (MesRuCl<sub>2</sub>)<sub>2</sub>, followed by strict Soxhlet extraction, led to the yolk–shell-mesostructured catalyst **5** as a dark-gray powder,

Key Laboratory of Resource Chemistry of Ministry of Education, Key Laboratory of Rare Earth Functional Materials, Shanghai Normal University, Shanghai 200234, China. E-mail: ghliu@shnu.edu.cn

† Electronic supplementary information (ESI) available: Experimental procedures and analytical data of chiral products. See DOI: 10.1039/c9cc07123g

‡ These authors contributed equally to this work.



Scheme 1 Preparation of catalyst 5.

where a similar catalyst 5' without  $\text{Fe}_3\text{O}_4$  on the yolk was also prepared by the reaction of 4' (obtained by the removal of  $\text{Fe}_3\text{O}_4$  from 4) and  $(MesRuCl_2)_2$  following a similar procedure (see Fig. S1 and S2 in the ESI†).

Through analysis of solid-state cross-polarization (CP)/magic angle spinning (MAS) spectra of 4' and 5' as representatives, the data clearly reveal the well-defined single-site active species in catalyst 5 (see Fig. S3 in the ESI†). It was found that material 4' and 5' have similar carbon signals for the chiral ligands, where the peaks at  $\delta = 64$ –68 ppm can be ascribed to alkyl carbon atoms, and those at  $\delta = 121$ –162 ppm correspond to aromatic carbon atoms in the  $-NCHC_6H_5$  moiety. Different from 4', the spectrum of catalyst 5' shows the appearance of new characteristic carbon signals at  $\delta = 20$  and 105 ppm, which are attributed to the methyl carbon atoms bonded to mesitylene and the aromatic carbon atoms in mesitylene. These signals in 5' are similar to those of its homologue  $MesRuTsDpen$ ,<sup>11a</sup> thereby confirming the well-defined single-site Ru/diamine centers in catalyst 5. The solid-state  $^{29}\text{Si}$  MAS NMR spectrum of catalyst 5' further demonstrates that catalyst 5 possesses an organic silica network with the strongest  $T^3$  species ( $R-Si(OSi)_3$ ;  $R =$  ethylene-bridged groups and/or alkyl-linked chiral functionalities) as its main silica wall of the outer silica shell, since the signals of the organic silica's T-series content in catalyst 5' were markedly higher than those of the inorganic silica's Q-series signals (see Fig. S4 in the ESI†).<sup>13</sup> This finding also suggests that the sandwiched inorganic  $\text{SiO}_2$ -coated layer has been mostly removed, guaranteeing the chiral Ru/diamine-functionality in the outer silica's nanochannels and the Pd/C particles on the inner magnetic yolk.

Fig. 1 presents the wide-angle XRD patterns and the magnetization curves of  $\text{Fe}_3\text{O}_4$ ,  $\text{SiO}_2@Pd/C@Fe_3O_4$  (1) and catalyst 5. The wide-angle XRD patterns (Fig. 1a) show the general diffraction peaks ( $2\theta$  values of 30.1, 35.4, 43.1, 57.0 and 62.6 degrees) of the  $\text{Fe}_3\text{O}_4$  nanoparticles, the characteristic diffraction peaks at ( $2\theta$  values of 40.0, 46.5 and 68.3 degrees) for the palladium composites in 1.<sup>14</sup> Due to the use of an *in situ* coating procedure, this comparison also suggests that the  $\text{Fe}_3\text{O}_4$  and palladium components in catalyst 5 could be retained.<sup>14c</sup> In addition, their magnetization saturation values are 60.85, 35.89, and 6.06  $\text{emu g}^{-1}$  (Fig. 1b), disclosing that catalyst 5 can be readily separated from the reaction system using an external magnet

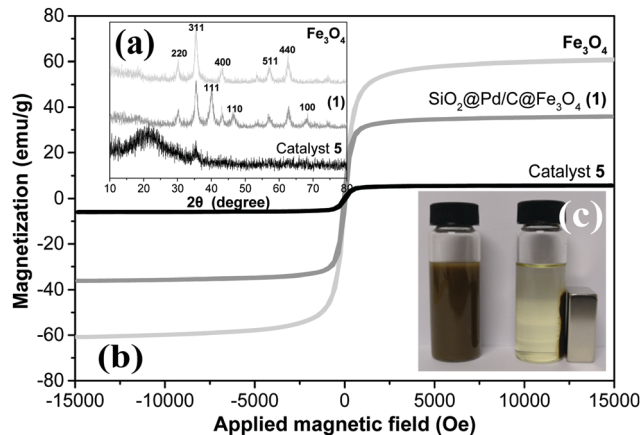
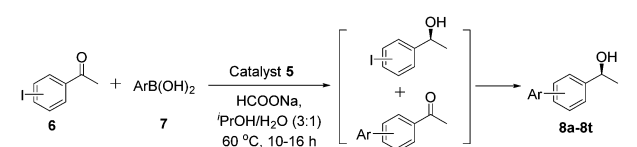


Fig. 1 (a) Wide-angle powder XRD patterns of  $\text{Fe}_3\text{O}_4$ ,  $\text{SiO}_2@Pd/C@Fe_3O_4$  (1) and catalyst 5. (b) Magnetization curves of  $\text{Fe}_3\text{O}_4$ ,  $\text{SiO}_2@Pd/C@Fe_3O_4$  (1) and catalyst 5 measured at 300 K. (c) Separation-redispersion images of catalyst 5 using an external magnet.

(Fig. 1c). In addition, the scanning electron microscopy (SEM) images revealed the uniformly dispersed nanoparticle with an average size of  $\sim 450$  nm, whereas transmission electron microscopy (TEM) demonstrated each silica yolk with  $\sim 250$  nm in diameter separated by a thin silica shell of  $\sim 80$  nm in thickness (see Fig. S5 in the ESI†). Nitrogen adsorption-desorption isotherm of catalyst 5 also disclosed its mesoporous structure owing to the existence of a typical IV character with an  $H_1$  hysteresis loop (see Fig. S5 in the ESI†).

With this magnetic catalyst 5 in hand, we initially investigated the single-step Suzuki cross-coupling reaction of 4-iodoacetophenone and phenylboronic acid to test the coupling ability of the Pd/C nanoparticles according to the optimal reaction conditions (see Table S1 in the ESI†).<sup>14a,15</sup> Firstly, we found that the mixed  $^1\text{PrOH}/\text{H}_2\text{O}$ -system (3:1, v/v) was able to produce the coupling intermediate 1-([1,1'-biphenyl]-4-yl)ethan-1-one in a quantitative yield. Then, this reaction system was also found to be compatible for the second-step ATH transformation, where the ATH of 1-([1,1'-biphenyl]-4-yl)ethan-1-one catalyzed by 5 provided (S)-1-([1,1'-biphenyl]-4-yl)ethan-1-ol with a slightly enhanced ee value relative to that catalyzed by its homologue  $MesRuTsDpen$  (97% yield and 99% ee *versus* 98% yield and 97% ee). Finally, when we combined the two single-step reactions into a one-pot Suzuki cross-coupling/ATH process, the reaction still provided the target chiral product in 96% yield with 99% ee, which is comparable to that attained with its parallel catalyst 5' (Table 1, entry 1 *versus* entry 1 in brackets). It is notable that the obtained enantioselectivity was slightly better than that obtained with a physical mixture of 4 and the homologue  $MesRuTsDpen$ , and markedly higher than that achieved *via* the physical mixing of Pd/C nanoparticles and  $MesRuTsDpen$  as dual catalysts (Table 1, entry 1 *versus* entries 2 and 3). These comparisons suggest that this active site-isolated feature in 5 enables the efficient elimination of the negative cross-interaction of the dual species, leading to enhanced reactivity and enantioselectivity.

Table 1 summarizes the general feasibility of the 5-catalyzed Suzuki cross-coupling/ATH cascade reactions of iodoacetophenones

Table 1 The 5-catalyzed Suzuki coupling/ATH cascade reactions<sup>a</sup>


Entry	I, 8	Ar	Yield <sup>b</sup> (%)	ee <sup>b</sup> (%)
1	4-I, 8a	Ph	96 (95)	99 (99) <sup>c</sup>
2	4-I, 8a	Ph	91	97 <sup>d</sup>
3	4-I, 8a	Ph	93	89 <sup>e</sup>
4	4-I, 8b	4-FPh	93	95
5	4-I, 8c	4-ClPh	97	94
6	4-I, 8d	3-ClPh	97	94
7	4-I, 8e	4-CF <sub>3</sub> Ph	93	94
8	4-I, 8f	3-CF <sub>3</sub> Ph	93	94
9	4-I, 8g	4-MePh	95	95
10	4-I, 8h	3-MePh	95	96
11	4-I, 8i	3-MeOPh	95	93
12	4-I, 8j	3-Thienyl	89	95
13	3-I, 8k	Ph	93	96
14	3-I, 8l	4-FPh	92	95
15	3-I, 8m	4-ClPh	92	95
16	3-I, 8n	3-ClPh	90	95
17	3-I, 8o	4-CF <sub>3</sub> Ph	95	95
18	3-I, 8p	4-MePh	94	95
19	3-I, 8q	3-MePh	92	95
20	3-I, 8r	3-MeOPh	97	94
21	3-I, 8s	3-Thienyl	84	95
22	4-I, 8t	4-AcetylPh	96	99 <sup>f</sup>

<sup>a</sup> Reaction conditions: catalyst 5 (21.98 mg, 2.0 μmol of Ru, 8.57 μmol of Pd, based on ICP analysis), HCO<sub>2</sub>Na (1.0 mmol), iodoacetophenones (0.10 mmol) and boronic acids (0.12 mmol), and 4.0 mL of (<sup>i</sup>PrOH/H<sub>2</sub>O, v/v = 3/1) were added sequentially to a 10.0 mL round-bottom flask. The mixture was then stirred at 60 °C for 10–16 h. <sup>b</sup> Yields were determined by <sup>1</sup>H-NMR analysis and ee values were determined by chiral HPLC analysis (see ESI in Fig. S8 and S11). <sup>c</sup> Data were obtained by the use of 5' as a catalyst. <sup>d</sup> Data were obtained from the use of a mixture of 4 and MesRuTsDpen as dual reductive catalysts. <sup>e</sup> Data were obtained from the use of a mixture of Pd/C nanoparticles and MesRuTsDpen as dual reductive catalysts. <sup>f</sup> dr value = 86/14.

and a series of aryl boronic acids. It was found that the various aryl boronic acids could efficiently react with 3- and 4-iodoacetophenone, providing the corresponding chiral biaryls in high yields and enantioselectivities. Also, the cascade reaction of acetylphenylboronic acid and 4-iodoacetophenone afforded (1*S*,1'*S*)-1,1'-([1,1'-biphenyl]-4,4'-diyl)bis(ethan-1-ol) in high yield with 99% ee and 96/14 dr (Table 1, entry 22).

Fig. 2 shows the kinetic process of the 5-catalyzed Suzuki cross-coupling/ATH of 4-iodoacetophenone and phenylboronic acid. Firstly, the Suzuki cross-coupling of 4-iodoacetophenone (6a) and phenylboronic acid (7a), and the asymmetric reduction of 6a proceed simultaneously as the concentration of 6a decreases sharply. During the first 2 h, a maximum transformation of 51% for the formation of reductive (*S*)-1-(4-iodophenyl)ethan-1-ol (A) and a maximum transformation of 20% for the formation of the coupling with 1-([1,1'-biphenyl]-4-yl)ethan-1-one (B) are observed. In the subsequent 2 h, the reaction proceeds rapidly to produce the chiral product (*S*)-1-(1,1'-biphenyl-4-yl)ethan-1-ol (8a). After that, the coupling of A and 7a, and the asymmetric reduction of B proceeds smoothly with the concomitant disappearance of A and B, providing 8a in 96% yield within 12 h. This time course shows a

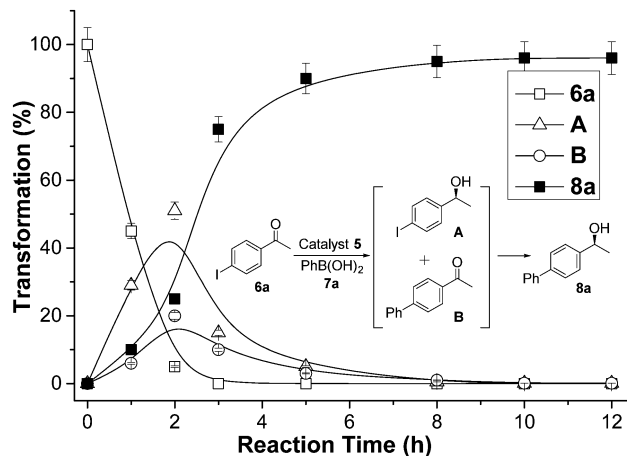
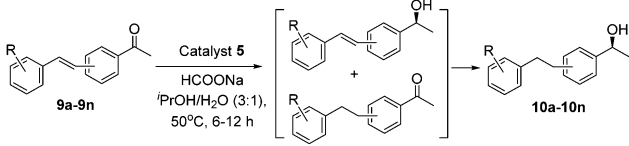


Fig. 2 Time course for the cascade reaction of 4-iodoacetophenone and phenylboronic acid catalyzed by 5.

synergistic Suzuki cross-coupling and ATH process in this cascade reaction.

Besides the utilization of the coupling ability of Pd/C nanoparticles, as shown in Table 1, the reducing ability of the Pd/C nanoparticles in catalyst 5 was also examined.<sup>8a</sup> Based on the obtained kinetic investigation of the successive reduction/ATH transformation of (*E*)-1-(4-styrylphenyl)ethanone (see Fig. S7 in the ESI<sup>†</sup>), Table 2 summarizes a series of 5-catalyzed cascade reactions, showing that all of the tested one-pot processes steadily provided the corresponding alkylethyl-substituted chiral aromatic alcohols in high yields with high enantioselectivities.

Fig. 3 exhibits the recycling of catalyst 5 in the Suzuki coupling/ATH cascade reactions of 4-iodoacetophenone and

Table 2 The 5-catalyzed successive reduction/ATH cascade reductions<sup>a</sup>


Entry	I, 8	Ar	Yield <sup>b</sup> (%)	Ee <sup>b</sup> (%)
1	4-, 10a	4-H	97	98
2	4-, 10b	4-F	94	94
3	4-, 10c	3-F	93	95
4	4-, 10d	4-Cl	95	96
5	4-, 10e	4-Me	95	96
6	4-, 10f	3-Me	94	96
7	4-, 10g	4-OMe	95	96
8	3-, 10h	4-H	93	96
9	3-, 10i	4-F	92	93
10	3-, 10j	3-F	92	94
11	3-, 10k	4-Cl	92	94
12	3-, 10l	4-Me	93	93
13	3-, 10m	3-Me	92	92
14	3-, 10n	4-OMe	93	95

<sup>a</sup> Reaction conditions: catalyst 5 (21.98 mg, 2.0 μmol of Ru, 8.57 μmol of Pd, based on ICP analysis), HCO<sub>2</sub>Na (1.0 mmol), ketones (0.10 mmol), and 4.0 mL of co-solvents (<sup>i</sup>PrOH/H<sub>2</sub>O v/v = 3/1) were added sequentially to a 10.0 mL round-bottom flask. The mixture was then stirred at 50 °C for 6–12 h. <sup>b</sup> The yields were determined by <sup>1</sup>H-NMR analysis and ee values were determined by chiral HPLC analysis (see ESI in Fig. S8 and S11).

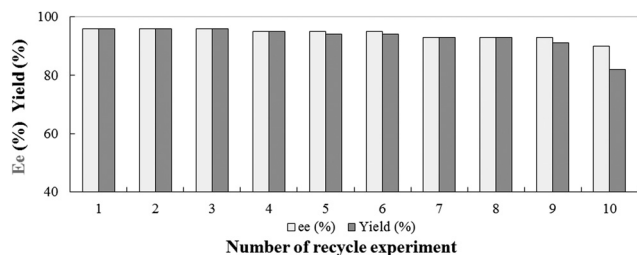


Fig. 3 Reusability of catalyst **5** in the Suzuki coupling/ATH cascade reactions of 4-iodoacetophenone and phenylboronic acid.

phenylboronic acid, where catalyst **5** was easily recovered using an external magnet that was placed near the reaction vessel. After nine consecutive runs, the recycled catalyst **5** still afforded the chiral products in 91% yield with 93% ee in the ninth run (see Table S2 and Fig. S9 in the ESI<sup>†</sup>). The obvious decrease in the yield in the tenth cycle (82% yield with 90% ee) can be attributed to the 11.3% of Ru loss detected by inductively coupled plasma optical emission spectrometry (ICP-OES) analysis, which led to the existence of more than 12% of the unconverted coupling intermediate. Similarly, catalyst **5** was also repeatedly recycled in the successive reduction/ATH enantioselective cascade reaction of (*E*)-1-(4-styrylphenyl)than-1-one after nine consecutive runs (see Table S3 and Fig. S10 in the ESI<sup>†</sup>).

In conclusion, we developed a yolk-shell-structured, magnetically retrievable bifunctional catalyst through the decoration of a Pd/C species onto the inner magnetic yolk and the chiral Ru/diamine species in the nanochannels of the outer silica shell. This bifunctional catalyst enables efficient Suzuki cross-coupling/asymmetric transfer hydrogenation of iodoacetophenones and aryl boronic acids *via* coupling and reduction processes, and the successive reduction/asymmetric transfer hydrogenation of the styryl-substituted aromatic ketones *via* the controllable reductions of the carbon-carbon and carbon-oxygen double bonds, providing various chiral products in high yields and enantioselectivities. The magnetic catalyst can also be conveniently recovered using an external magnet and repeatedly recycled, showing that it is practical for use in real applications.

We are grateful to the China National Natural Science Foundation (21672149) for financial support.

## Conflicts of interest

There are no conflicts to declare.

## Notes and references

- (a) S. Shylesh, V. Schünemann and W. R. Thiel, *Angew. Chem., Int. Ed.*, 2010, **49**, 3428–3459; (b) V. Polshettiwar, R. Luque, A. Fihri, H. Zhu, M. Bouhrara and J. M. Basset, *Chem. Rev.*, 2011, **111**, 3036–3075; (c) M. B. Gawande, P. S. Branco and R. S. Varma, *Chem. Soc. Rev.*, 2013, **42**, 3371–3393.

- (a) Y. H. Liu, J. Deng, J. W. Gao and Z. H. Zhang, *Adv. Synth. Catal.*, 2012, **354**, 441–447; (b) V. Polshettiwar and R. S. Varma, *Org. Biomol. Chem.*, 2009, **7**, 37–40; (c) S. Byun, J. Chung, Y. Jang, J. Kwon, T. Hyeon and B. M. Kim, *RSC Adv.*, 2013, **3**, 16296–16299; (d) R. Arundhathi, D. Damodara, P. R. Likhar, M. L. Kantam, P. Saravanan, T. Magdaleno and S. H. Kwon, *Adv. Synth. Catal.*, 2011, **353**, 1591–1600; (e) R. Luque, B. Baruwati and R. S. Varma, *Green Chem.*, 2010, **12**, 1540–1543; (f) R. B. Nasir Baig and R. S. Varma, *Green Chem.*, 2012, **14**, 625–632; (g) D. Wang, L. Salmon, J. Ruiz and D. Astruc, *Chem. Commun.*, 2013, **49**, 6956–6958; (h) G. Chouhan, D. Wang and H. Alper, *Chem. Commun.*, 2007, 4809–4811.
- (a) M. L. Kantam, J. Yadav, S. Laha, P. Srinivas, B. Sreedhar and F. Figueras, *J. Org. Chem.*, 2009, **74**, 4608–4611; (b) O. Gleeson, R. Tekoriute, Y. K. Gun'ko and S. J. Connon, *Chem. – Eur. J.*, 2009, **15**, 5669–5673; (c) A. Hu, T. Gordon, G. T. Yee and W. Lin, *J. Am. Chem. Soc.*, 2005, **127**, 12486–12487; (d) V. S. Ranganath, J. Kloesges, A. H. Schafer and F. Glorius, *Angew. Chem., Int. Ed.*, 2010, **49**, 7786–7789; (e) B. Panella, A. Vargas and A. Baiker, *J. Catal.*, 2009, **261**, 88–93; (f) T. Zeng, L. Yang, R. Hudson, G. Song, A. R. Moores and C. J. Li, *Org. Lett.*, 2011, **13**, 442–445; (g) D. Lee, J. Lee, H. Lee, S. Jin, T. Hyeon and B. M. Kim, *Adv. Synth. Catal.*, 2006, **348**, 41–46.
- (a) C. Perego and R. Millini, *Chem. Soc. Rev.*, 2013, **42**, 3956–3976; (b) C. Li, H. Zhang, D. Jiang and Q. Yang, *Chem. Commun.*, 2007, 547–558.
- S. W. Jun, M. Shokouhimehr, D. J. Lee, Y. Jang, J. Park and T. Hyeon, *Chem. Commun.*, 2013, **49**, 7821–7823.
- (a) N. Ma, Y. Deng, W. Liu, S. Li, J. Xu, Y. Qu, K. Gan, X. Sun and J. Yang, *Chem. Commun.*, 2016, **52**, 3544–3547; (b) Y. Chen, Q. Meng, M. Wu, S. Wang, P. Xu, H. Chen, Y. Li, L. Zhang, L. Wang and J. Shi, *J. Am. Chem. Soc.*, 2014, **136**, 16326–16334; (c) H. Djojoputro, X. F. Zhou, S. Z. Qiao, L. Z. Wang, C. Z. Yu and G. Q. Lu, *J. Am. Chem. Soc.*, 2006, **128**, 6320–6321.
- (a) T. Cheng, D. Zhang, H. Li and G. Liu, *Green Chem.*, 2014, **16**, 3401–3427; (b) Y. Sun, G. Liu, H. Gu, T. Huang, Y. Zhang and H. Li, *Chem. Commun.*, 2011, **47**, 2583–2585; (c) X. Gao, R. Liu, D. Zhang, M. Wu, T. Cheng and G. Liu, *Chem. – Eur. J.*, 2014, **20**, 1515–1519.
- (a) Y. Su, F. Chang, R. Jin, R. Liu and G. Liu, *Green Chem.*, 2018, **20**, 5397–5540; (b) J. Y. Xu, T. Y. Cheng, K. Zhang, Z. Y. Wang and G. H. Liu, *Chem. Commun.*, 2016, **52**, 6005–6008.
- (a) F. X. Felpin, *Synlett*, 2014, 1055–1067; (b) Y. Li, Z. Zhang, J. Shen and M. Ye, *Dalton Trans.*, 2015, **44**, 16592–16601; (c) M. J. Jin and D. H. Lee, *Angew. Chem., Int. Ed.*, 2010, **49**, 1119–1122.
- (a) X. Wu, J. Liu, D. D. Tommaso, J. A. Iggo, C. R. A. Catlow, J. Bacsá and J. Xiao, *Chem. – Eur. J.*, 2008, **14**, 7699–7715; (b) K. Matsumura, S. Hashiguchi, T. Ikariya and R. Noyori, *J. Am. Chem. Soc.*, 1997, **119**, 8738–8739.
- (a) S. Hashiguchi, A. Fujii, J. Takehara, T. Ikariya and R. Noyori, *J. Am. Chem. Soc.*, 1995, **117**, 7562–7563; (b) T. Ohkuma, K. Tsusumi, N. Utsumi, N. Arai, R. Noyori and K. Murata, *Org. Lett.*, 2007, **9**, 255–257.
- (a) Z. Sun, J. Yang, J. Wang, W. Li, S. Kaliaguine, X. Hou, Y. Deng and D. Zhao, *J. Mater. Chem. A*, 2014, **2**, 6071–6074; (b) T. Yao, T. Cui, X. Fang, F. Cui and J. Wu, *Nanoscale*, 2013, **5**, 5896–5904; (c) J. Dai, H. Zou, R. Wang, Y. Wang, Z. Shi and S. Qiu, *Green Chem.*, 2017, **19**, 1336–1344.
- O. Kröcher, R. A. Köppel, M. Fröba and A. Baiker, *J. Catal.*, 1998, **178**, 284–298.
- (a) M. Zhu and G. Diao, *J. Phys. Chem. C*, 2011, **115**, 24743–24749; (b) L. Kong, X. Lu, X. Bian, W. Zhang and C. Wang, *ACS Appl. Mater. Interfaces*, 2011, **3**, 35–42; (c) J. Dai, H. Zou, R. Wang, Y. Wang, Z. Shi and S. Qiu, *Green Chem.*, 2017, **19**, 1336–1344.
- (a) Z. Sun, J. Yang, J. Wang, W. Li, S. Kaliaguine, X. Hou, Y. Deng and D. Zhao, *J. Mater. Chem. A*, 2014, **2**, 6071–6074; (b) R. K. Sharma, S. Dutta, S. Sharma, R. Zboril, R. S. Varma and M. B. Gawande, *Green Chem.*, 2016, **18**, 3184–3209; (c) Y. Zhang, Y. Yang, H. Duan and C. Lu, *ACS Appl. Mater. Interfaces*, 2018, **10**, 44535–44545; (d) Q. L. Fang, Q. Cheng, H. Xu and S. Xuan, *Dalton Trans.*, 2014, 43(2588), 2588–2595; (e) S. Omar and R. Abu-Reziq, *J. Phys. Chem. C*, 2014, **118**, 30045–30056.